

## General Disclaimer

### One or more of the Following Statements may affect this Document

- This document has been reproduced from the best copy furnished by the organizational source. It is being released in the interest of making available as much information as possible.
- This document may contain data, which exceeds the sheet parameters. It was furnished in this condition by the organizational source and is the best copy available.
- This document may contain tone-on-tone or color graphs, charts and/or pictures, which have been reproduced in black and white.
- This document is paginated as submitted by the original source.
- Portions of this document are not fully legible due to the historical nature of some of the material. However, it is the best reproduction available from the original submission.

# PRECISION ORBIT COMPUTATIONS FOR STARLETTE

*Tmx-71303*

**JAMES G. MARSH  
RONALD G. WILLIAMSON**

(NASA-TM-X-71303) PRECISION ORBIT  
COMPUTATIONS FOR STARLETTE (NASA) 27 p  
HC A03/MF A01 CSCL 22A

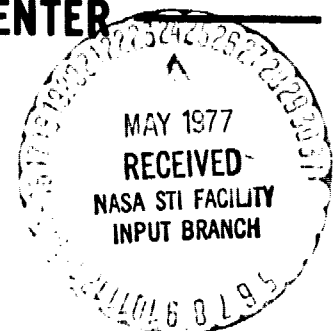
N77-23141

Unclas  
G3/13 28942

DECEMBER 1976

**GSFC**

**GODDARD SPACE FLIGHT CENTER  
GREENBELT, MARYLAND**



**PRECISION ORBIT COMPUTATIONS**  
**FOR STARLETTE**

**James G. Marsh**

**Geodynamics Branch  
Goddard Space Flight Center  
Greenbelt, Maryland**

**Ronald G. Williamson**

**Wolf Research and Development Group  
EG&G/Washington Analytical Services Center, Inc.  
6801 Kenilworth Avenue  
Riverdale, Maryland**

**Presented at the  
Fall Meeting of the  
American Geophysical Union  
San Francisco, California**

**December 6-10, 1976**

**GODDARD SPACE FLIGHT CENTER  
Greenbelt, Maryland**

PRECISION ORBIT COMPUTATIONS  
FOR STARLETTE

James G. Marsh

Geodynamics Branch  
Goddard Space Flight Center  
Greenbelt, Maryland

Ronald G. Williamson

Wolf Research and Development Group  
EG&G/Washington Analytical Services Center, Inc.  
6801 Kenilworth Avenue  
Riverdale, Maryland

ABSTRACT

The Starlette satellite, launched in February 1975 by the French Centre National d'Etudes Spatiales, was designed to minimize the effects of non-gravitational forces and to obtain the highest possible accuracy for laser range measurements. Analyses of the first four months of global laser tracking data have confirmed the stability of the orbit and the precision to which the satellite's position can be established.

Initial orbit computations using the GSFC GEM-7 gravity model produced rms fits of about 8 to 10 meters for arc lengths of 5 days. Through a series of gravity model improvements these rms fits have been reduced to 1 to 2 meters for the 5 day arcs. An rms fit of 4.3 meters was obtained for a 90 day arc. Five day arcs overlapped by 2.5 days showed rms satellite position differences generally less than 2 meters. Prediction errors at the end of two months were less than 30 milliseconds.

## CONTENTS

	<u>Page</u>
ABSTRACT . . . . .	111
INTRODUCTION . . . . .	1
LASER TRACKING DATA . . . . .	2
ORBITAL PERTURBATIONS . . . . .	3
ORBIT COMPUTATIONS . . . . .	6
CONCLUSIONS . . . . .	11
ACKNOWLEDGMENTS . . . . .	11
REFERENCES . . . . .	12

## ILLUSTRATIONS

<u>Figure</u>		<u>Page</u>
1	Starlette Laser Range Residuals Single Pass . . . . .	14
2	Starlette Semi-Major Axis Perturbations . . . . .	15
3	Starlette Inclination Perturbations Based Upon $k_2$ Love Number = 0.3 . . . . .	15
4	Starlette Node Perturbations . . . . .	16
5	Starlette - RMS of Fit as a Function of Arc Length . . . . .	17
6	Starlette Ninety Day Orbit Timing Errors At The Arequipa, Peru Laser Station . . . . .	18
7	Starlette Ninety Day Orbit Range Biases at the Arequipa, Peru Laser Station . . . . .	19

## ILLUSTRATIONS (Continued)

<u>Figure</u>		<u>Page</u>
8	Starlette Orbit Prediction Based Upon A Five Day Arc Timing Errors At The Arequipa, Peru Laser Station . . . . .	20
9	Starlette Orbit Prediction Based Upon a Five Day Arc Range Biases At The Arequipa, Peru Laser Station . . . . .	21

## TABLES

<u>Table</u>		<u>Page</u>
1	Starlette Gravity Model Comparison RMS Fits for 5-Day Orbits . . . . .	22
2	Gravity Model Effects on Orbit Overlap RMS Differences (Meters) (5-Day Orbits With a 2.5 Day Overlap) . . . . .	22
3	Statistics by Station for Starlette 90 Day Arc May 1 to August 1, 1975 . . . . .	23

# PRECISION ORBIT COMPUTATIONS FOR STARLETTE

## INTRODUCTION

On February 6, 1975 the Starlette satellite was launched by the French Centre National d'Etudes Spatiales (CNES). Tracking and orbit computation accuracies since achieved indicate that this satellite is of major significance to geophysical and geodetic analyses.

Starlette (CNES/GRGS, 1975) was designed to obtain the highest possible accuracy for laser range measurements and to minimize the effects of non-gravitational forces. The satellite was designed to be a high density specularly reflecting sphere having a radius of 12 cm and a weight of 47.295 kg. The low area to mass ratio was achieved by using a core which is largely uranium 238. The skin is an aluminum alloy containing a total of 60 laser corner reflectors. The orbit selected has an inclination of  $49.8^\circ$  and is well above the high drag region, having normal apogee and perigee heights of 1105 and 810 km, respectively.

To determine the contribution Starlette might provide to our studies, we began an in-depth analysis of all available precision reduced laser data in the April to August 1975 period. The data were from the CNES, Smithsonian Astrophysical Observatory (SAO), and Goddard Space Flight Center (GSFC) systems. The objectives of the analyses were to assess the stability and accuracy of the orbit, the quality of the laser tracking data, the accuracy of our presently adopted

set of geodetic constants and force models, and the amount of improvement which could be readily accomplished by using these data to improve our estimate of the coefficients in the models. The results of these analyses to date are presented in detail in the following sections.

#### LASER TRACKING DATA

A total of 809 passes of precision reduced laser data were available for the period of March through August 1975. A large percentage of these data were recorded by the SAO stations. In June the total of nine stations tracking contributed typically eight to ten passes of data per day. On numerous occasions the SAO stations at Arequipa, Peru and Olifantsfontein Republic of S. Africa observed three passes per day. Thus, a substantial amount of laser data is available.

The GSFC data have been preprocessed using a program developed by Carpenter (1976). Extensive analyses of these data by Carpenter during the preprocessing stage have indicated that the precision is on the order of 10 cm or better. While we have not conducted an extensive short arc analysis of the data from the other stations, the internal consistency of the data in long arc orbits from Arequipa, Olifantsfontein, Mt. Hopkins, Arizona and Natal, Brazil is on the order of 50 to 150 cm, and is typically 100 to 200 cm for the Greece station and the CNES station in the Canary Islands.



Data rates for the respective systems are: CNES - every four seconds, SAO - every 7.5 seconds except for the SAO/National Technical University of Athens laser - once per 30 seconds, GSFC - once per second. A typical set of residuals for a GSFC site is presented in Figure 1.

## ORBITAL PERTURBATIONS

To evaluate the nominal behavior of the Starlette orbit, both an analytic gravitational harmonic analysis approach and a long periodic semi-analytic approach were used.

The gravitational harmonic analysis approach, embodied as the Harmonic Analysis Program (HAP) computer program, computes the expected perturbation amplitudes associated with each specific frequency in the orbit (i.e., argument of perigee, right ascension of the node, mean anomaly). The formulation is taken from Kaula (1966, Eq. 3.76). This is a linear theory based on analytic integration of the Lagrange Planetary Equations over a cycle of the particular orbit-referred driving frequency under the assumption that the elements and rates are constant over the interval. HAP also assumes the  $J_2$  secular rates sufficiently represent the total rates. The program uses either a specific gravity field or Kaula's "rule of thumb" as an estimate of the coefficient values:

$$\sigma\{\bar{C}_{\ell m}, \bar{S}_{\ell m}\} \approx 10^{-5}/\ell^2$$

This rule of thumb was developed by Kaula from auto-covariance analysis of gravimetry and has proved remarkably successful.

The  $J_2$  rates on Starlette indicate that the orbit has a fairly short perigee period of about 110 days, with the observable periods of the zonal perturbations being around 110, 55, 37, and 27 days. The nodal period is also fairly short, being around 91 days. The nodal period with respect to the sun is about 73 days. Taking into account orbit plane symmetry, we would expect to observe solar perturbations with a frequency of around  $73/2 \approx 37$  days which is close to the  $|q| = 3$  zonal frequency and hence with certain kinds of analyses, drag or zonal error will resemble solar perturbations.

These HAP analyses indicate that the primary resonance perturbations have beat periods around 2.7 days due to  $14^{\text{th}}$  order terms of the geopotential. When Kaula's rule is used to approximate the geopotential, an along track effect of about 50 to 100 meters is predicted for these  $14^{\text{th}}$  order terms. Similar results are obtained when the GEM-7 geopotential coefficients (Wagner et al., 1976) are used. In addition to the  $14^{\text{th}}$  order resonance, there is a sideband resonance with  $13^{\text{th}}$  order terms having a beat period of around 1.5 days whose effect along track is in excess of 10 m. The possibility also exists for being able to observe the double resonance with  $28^{\text{th}}$  order terms which have beat periods of around 1.3 days.

The non-resonant perturbations are generally less than one meter along track for the coefficients above (12, 12). However, some higher degree coefficients, for example (14, 10), produce effects larger than a meter. Even above (15, 15), 10 cm effects are typically observed.

In order to evaluate the perturbations due to atmospheric drag, direct solar radiation pressure, lunar and solar solid body tides and the lunar and solar direct gravitational effects, we employed a long periodic semi-analytic program, the "Rapid Orbit Analysis and Determination" program (Wagner et al., 1974). ROAD numerically integrates the long periodic orbit and variational equations. The ROAD formulation of the potential is similar to that presented in Kaula (1966) with the short period variations removed. The above perturbations were investigated by comparing orbits with and without the desired perturbation over the time span for which we had data. The initial conditions are identical so there will be some slight energy discrepancy.

Figures 2, 3, and 4 present the computed effects of these forces on the semi-major axis, inclination and the right ascension of the ascending node. The direct luni-solar perturbations are qualitatively like the tides except for a scale factor and thus were intentionally omitted from the graphs.

Over the three month time period, drag reduces the semi-major axis by about 1.5 meters while radiation pressure causes an increase of about 0.5 meters. Radiation pressure produces a maximum perturbation of 0.02 arcseconds in the inclination while the drag effects of less than  $10^{-3}$  arcseconds are insignificant. By comparison, the tidal perturbations are on the order of an arcsecond. In the node, radiation pressure and drag produce perturbations of about equal magnitude (0.4 arcseconds) but with opposite signs. Tidal perturbations in the node are on the order 1 to 3 arcseconds.

As shown in Figures 2, 3 and 4, the perturbing forces produce very different effects in the semi-major axis, inclination and node. This fact facilitates separability of the recovered effects when the different elements are used together in a solution. Over a longer time span the periodic nature of the solar radiation pressure perturbation would become evident.

Errors in the zonal harmonic coefficients may also produce long periodic errors in the node. An assessment of the magnitude of this error source is required.

## ORBIT COMPUTATIONS

For detailed analysis of the Starlette laser data, we used the GEODYN (Martin, 1972) orbit and geodetic parameter estimation computer program. The program employs an 11<sup>th</sup> order Cowell numerical integration procedure. Satellite disturbing forces modeled in the program included the gravity field of the earth in the form of spherical harmonic coefficients, third-body gravitation, atmospheric drag, luni-solar solid-earth tides and direct solar radiation pressure. For the lunar and solar positions required in the computation of the third-body gravitational effects, the Jet Propulsion Laboratory ephemeris DE-69 was used. The atmospheric density was modeled using either the Jacchia model atmospheres (Jacchia 1965, 1970, 1971, Jacchia et al, 1968).

For the initial analyses, the data set was divided into consecutive 5 day arcs. This arc length was selected because it corresponds approximately to two resonant

beat periods and would enable us to investigate the adequacy of the resonant coefficient modeling. The orbit determinations were performed using the GEM-7 and GEM-8 gravity models (Wagner, et al., 1976), the GSFC 1973 station coordinates (Marsh, et al., 1973), and the 1965 Jacchia atmosphere.

Rms fits as large as 16 meters were observed when the GEM-8 model was used and almost 11 meters when GEM-7 was used, with both models demonstrating a considerable variation from arc to arc. Analysis of the pass by pass timing biases for some sample arcs clearly demonstrated the resonance period of about 2.7 days.

Resonant coefficients for 13<sup>th</sup>, 14<sup>th</sup> and 28<sup>th</sup> order terms in the GEM-7 model were adjusted in a multi-arc solution with 19 consecutive 5 day arcs in the March to June period. The rms fit for each arc was generally reduced by a factor of two or more to an overall level of about 4 meters. The fits were also significantly more stable from arc to arc.

For a measure of orbit error other than the regression statistics, we computed radial, cross-track and along-track position differences between the orbits associated with each gravity model. The average rms position differences between the GEM-7 and GEM-8 orbits were 3 to 4 meters for radial and cross-track components and about 13 meters along-track. A comparison of orbits produced by the GEM-7 model containing the adjusted resonance coefficients with

those obtained from GEM-7 showed effects of similar magnitude. The rms differences between the modified GEM-7 orbits and the GEM-8 orbits were larger by almost 50%.

The overall level of the rms of fit produced in the data reductions using the GEM-7 modified gravity model was too large to be explained by anything other than geopotential mismodeling. Fortunately, the global distribution of high quality laser data well distributed over a full revolution of the argument of perigee provided the opportunity to derive a gravity model which was tailored to Starlette. By combining the normal equations produced from 26 five day Starlette arcs with the complete GEM-7 normal equations, we were able to adjust a complete GEM-7 size field. The model chosen after several investigations has been designated as PGS-ST4. Table 1 presents rms fits for several five day arcs in June 1975 which are typical of the level of fit of the tailored model. Whereas the GEM-7 model produced rms fits on the order of 10 meters, the PGS-ST4 model produced rms fits of 1 to 2 meters.

To assess the relative consistency of the GEM-7 and PGS-ST4 orbits, the technique of overlapping orbits was employed. Table 2 presents rms radial, cross-track and along-track orbit differences for five day orbits overlapped by two and a half days. The rms along-track differences for the PGS-ST4 orbits are less than 2 meters while differences as large as 18 meters are noted for the GEM-7 model. Radially, the consistency of the orbits has been considerably

improved from a maximum of 3 meters to less than 40 cm. The cross-track differences were also reduced when the PGS-ST4 model was used but not as substantially.

Because the PGS-ST4 gravity model was derived using five day arcs and the previously discussed tests also used five day arcs, arcs in lengths of two, thirty-five, sixty-six and ninety days were also evaluated. For these investigations, the Jacchia 1971 model atmosphere was used. Drag and solar radiation pressure coefficients were adjusted in the thirty-five day and longer arcs. The degradation in the rms fit as a function of the increased arc lengths was approximately linear as is shown in Figure 5, reaching a value of only 4.3 meters after ninety days.

The ninety day arc is probably of most interest because it represents a full period of the dominant unmodeled perturbation (the  $K_1$  ocean tide). Table 3 presents a breakdown of the statistics by station for this arc. There are a total of over 540 passes of data from nine stations. The effects of the different system noise levels in the SAO and GSFC data is clearly evident in the statistics. To demonstrate the consistency in this ninety day orbit, timing errors and range biases were calculated from the residuals for each pass of data. Figures 6 and 7 present the results of these calculations for the Arequipa station which had very good coverage throughout the arc. Timing errors were generally less than 2 milliseconds and the range biases were less than five meters. Plots for the

other stations are similar in character. The causes for these residual patterns are currently under investigation.

Orbit prediction capability is also of great importance for the laser geodynamics satellites. The GSFC lasers have narrow beam widths,  $1/3$  milliradian, and acquisition is difficult if the predictions contain large errors. Furthermore, in the past it has been necessary to update the predictions on a weekly basis for satellites such as BE-C, GEOS-1, GEOS-2, and GEOS-3.

To test the prediction capabilities of the PGS-ST4 gravity model, timing errors and range biases were investigated for a five day orbit propagated over a two month period. Initially the orbit was propagated using nominal values for drag and solar radiation pressure. At the end of the two month period the timing error calculated at Arequipa reached a value of nearly 200 milliseconds. Using more representative drag and solar radiation pressure values (derived from a 35 day arc), the timing errors at the end of the period were reduced to about 30 milliseconds and the range biases were less than 15 meters. Plots of these timing errors and the range biases over this period are shown in Figures 8 and 9. This small prediction error is unparalleled in our previous experience. For example, prediction error for the BE-C satellite at the end of 60 days would be on the order of seconds.



## CONCLUSIONS

These analyses of the Starlette laser tracking data have shown that by simply improving the gravity model, rms fits of a few meters can be achieved for arc lengths as long as ninety days. The consistency of five day orbits is a few tens of centimeters radially and less than two meters along-track. Prediction errors at the end of two months are reducible to under 30 milliseconds. Any significant improvement will necessarily come from model improvement in the area of tides, polar motion, and other subtle geodynamic effects.

Continued laser tracking data are expected to provide a strong complement to the GEOS-III tracking data for a global center of mass adjustment of the tracking station coordinates. Analyses of the long term evolution of the orbit should provide significant contributions to studies of earth and ocean tides. As more data are collected, contributions to tectonic motion, polar motion and earth rotation studies should be realized.

## ACKNOWLEDGMENTS

The authors thank Neader Boulware for executing the orbit computation runs, Frank Lerch and Bill Wells for their valuable discussions on the adjustment of the gravity model, and Jim Richardson and Dan McCormick for their help in executing the gravity model adjustments.

## REFERENCES

1. Carpenter, L. , "Laser Tracking Data Processing," EOS Transactions of the American Geophysical Union, Volume 57, No. 4, p. 235, 1976.
2. Centre National d'Etudes Spatiales, Groupe De Recherches de Geodesie Spatiale, "Starlette," Toulouse, France, February 1975.
3. Jacchia, L. G. , "Static Diffusion Models of the Upper Atmosphere with Empirical Temperature Profiles," SAO Spec. Rep. 170, Smithson. Inst. Astrophys. Observ. , Cambridge, Mass. , 1965.
4. Jacchia, L. G. , "New Static Models of the Thermosphere and Exosphere with Empirical Temperature Profiles," SAO Spec. Rep. 313, Smithson. Inst. Astrophys. Observ. , Cambridge, Mass. , 1970.
5. Jacchia, L. G. , "Revised Static Models of the Thermosphere and Exosphere with Empirical Temperature Profiles," SAO Spec. Rep. 332, Smithson. Inst. Astrophys. Observ. , Cambridge, Mass. , 1971.
6. Jacchia, L. G. , Campbell, I. G. , and Slowley, J. W. , "Semi-Annual Density Variations in the Upper Atmosphere," 1958 to 1966, SAO Spec. Rep. 265, Smithson. Inst. Astrophys. Observ. , Cambridge, Mass. , 1968.
7. Kaula, W. M. , "Theory of Satellite Geodesy," Blaisdell Publishing Company, Waltham, Mass. , 1966.
8. Marsh, J. G. , Douglas, B. C. , and Klosko, S. M. , "A Global Station Coordinate Solution Based Upon Camera and Laser Data - GSFC-1973," Proceedings of the International Symposium on the Use of Artificial Satellites

for Geodesy and Geodynamics, National Technical University, Athens,  
pp. 749-799, 1973.

9. Martin, T. V., "GEODYN Systems Operations Description," Final Report on Contract NAS 5-11736-129, WOLF Research and Development Corp., Riverdale, Md., February 1972.
10. Wagner, C. A., Douglas, B. C., Williamson, R. G., "The ROAD Program," GSFC Document X-921-74-144, 1974.
11. Wagner, C. A., Lerch, F. J., Brownd, J. E., Richardson, J. A., "Improvement in the Geopotential Derived from Satellite and Surface Data (GEM-7 and -8)," Journal of Geophysical Research, 82, No. 5, pp. 901-914, 1977.

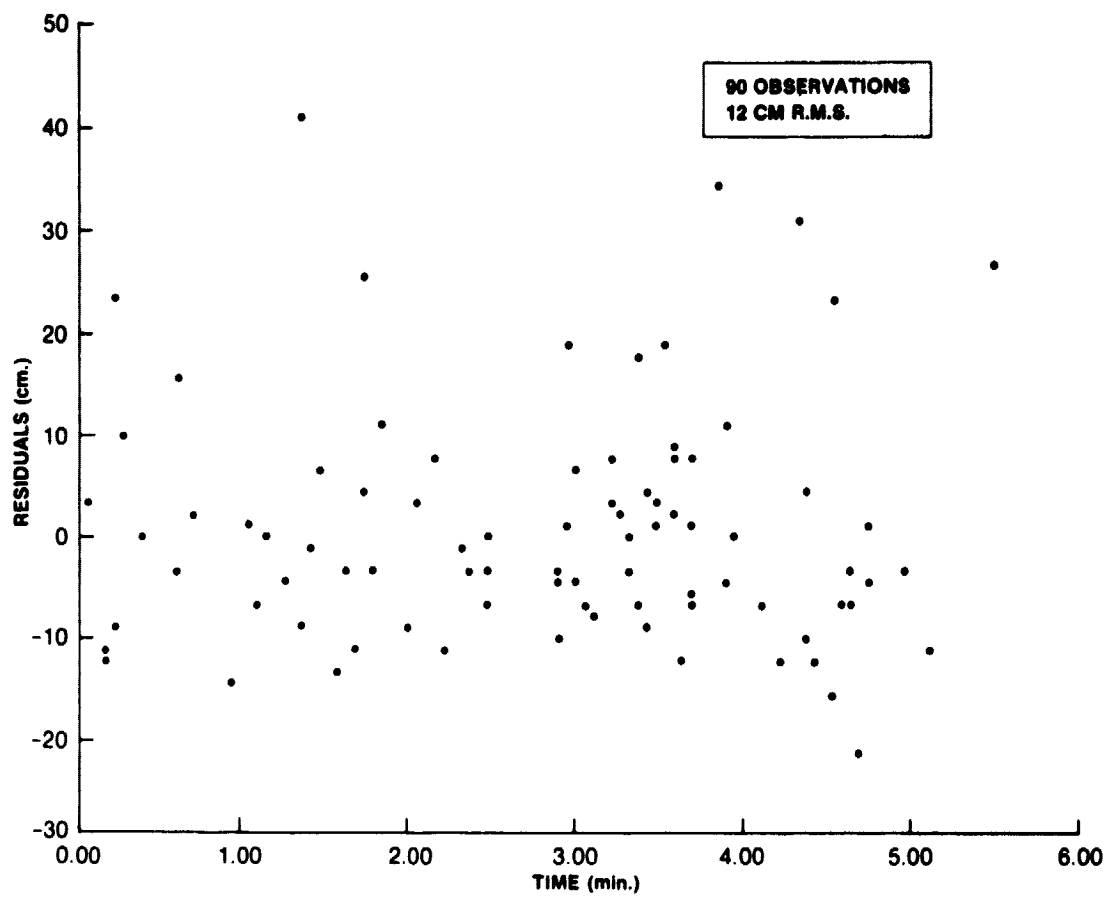


Figure 1. Starlette Laser Range Residuals Single Pass

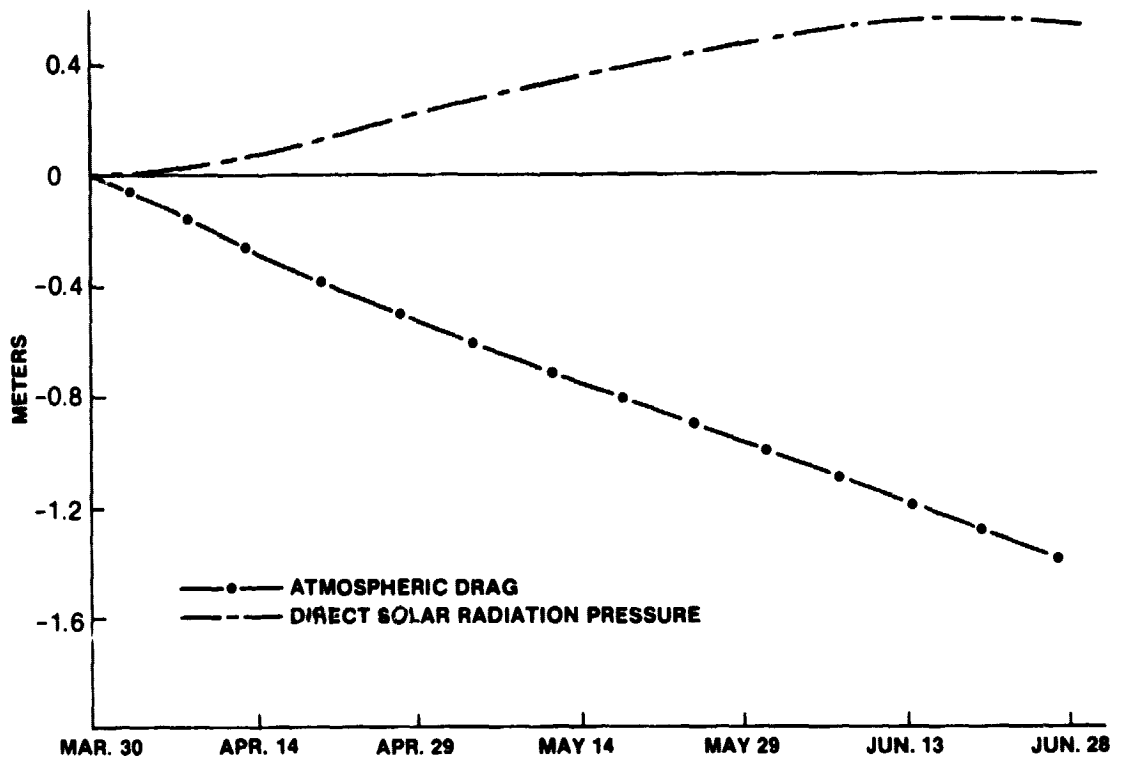


Figure 2. Starlette Semi-Major Axis Perturbations

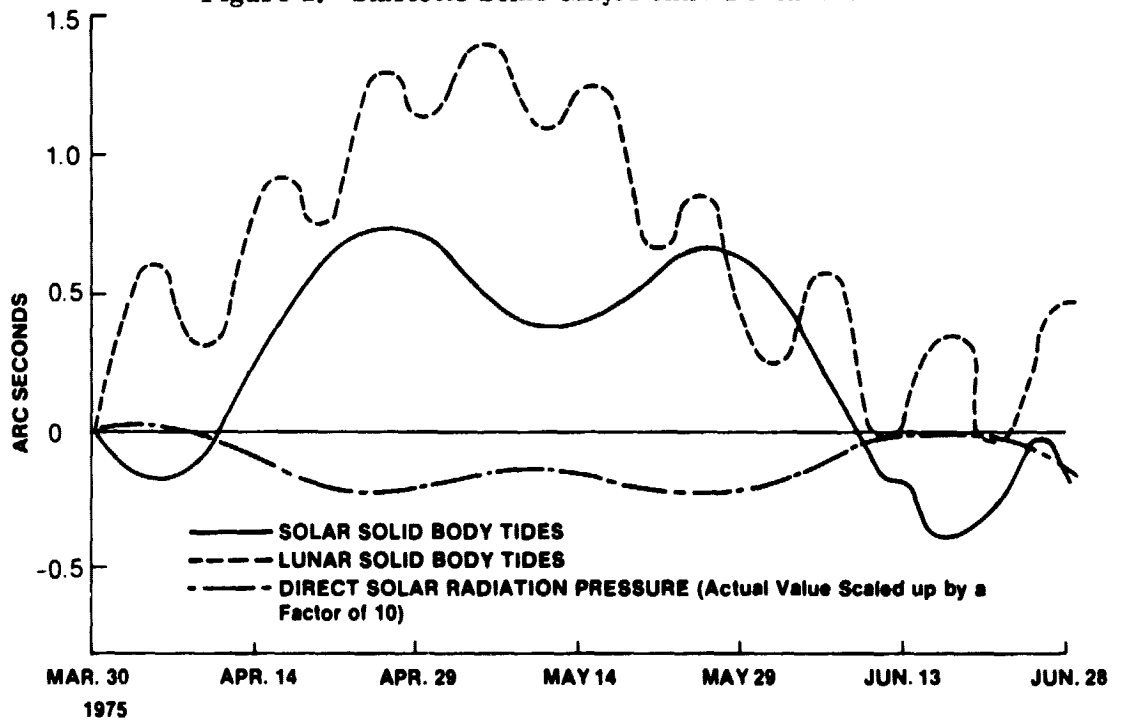


Figure 3. Starlette Inclination Perturbations Based Upon  $k_2$  Love Number = 0.3

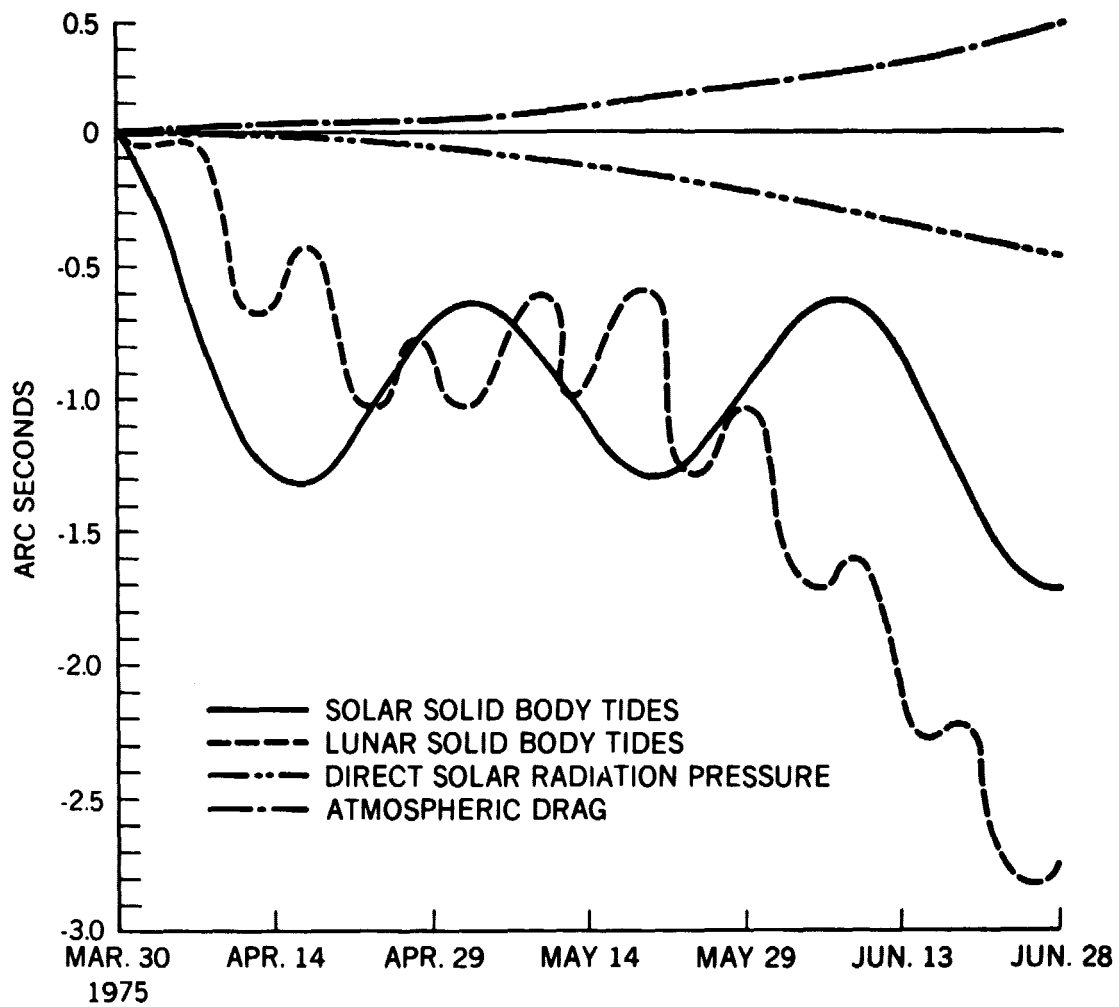


Figure 4. Starlette Node Perturbations

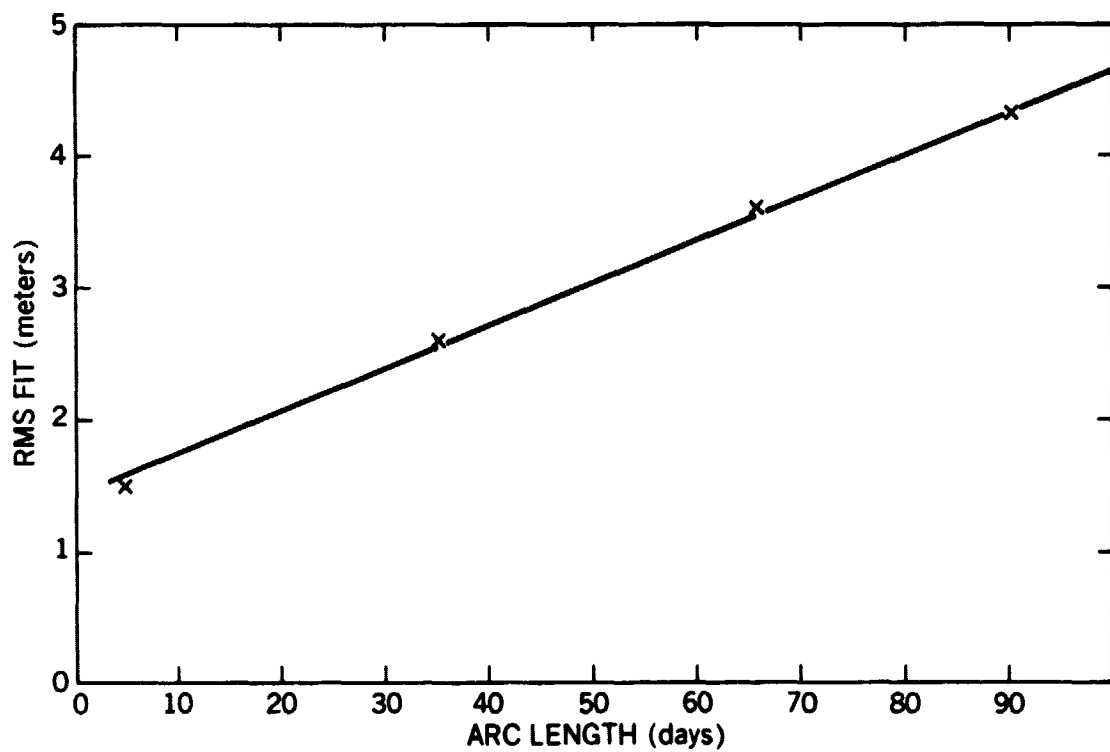
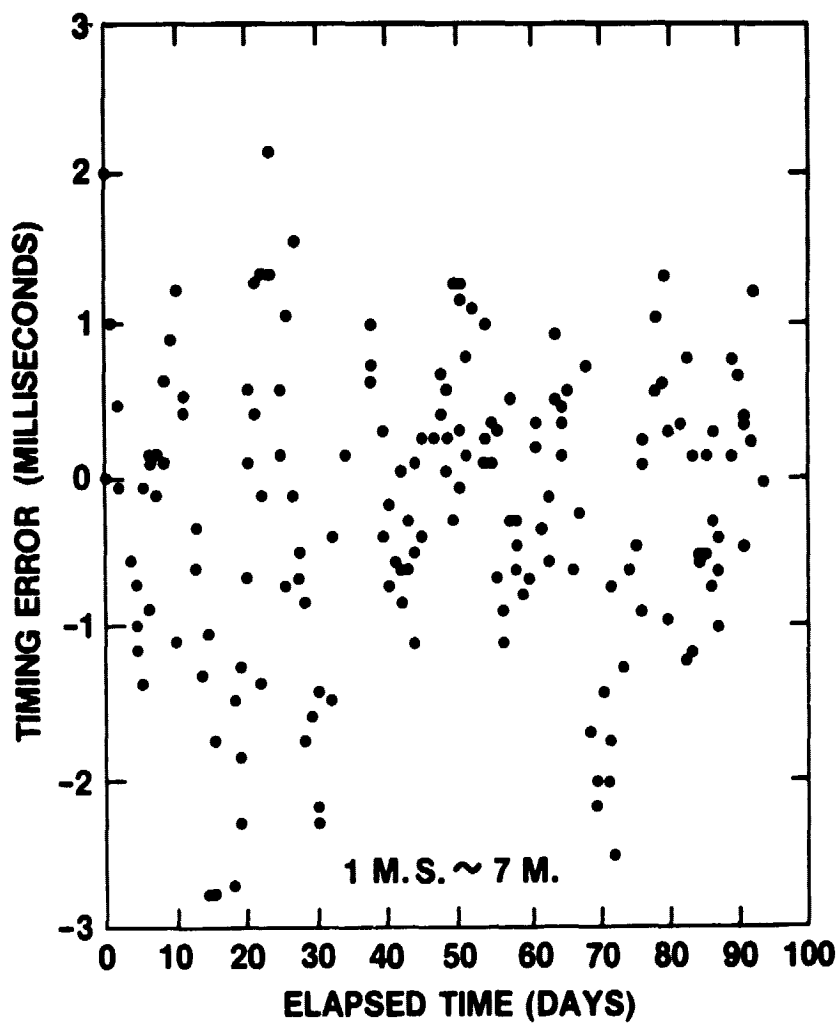


Figure 5. Starlette - RMS of Fit as a Function of Arc Length



JUNE 26, 1975

Figure 6. Starlette Ninety Day Orbit Timing Errors  
At The Arequipa, Peru Laser Station



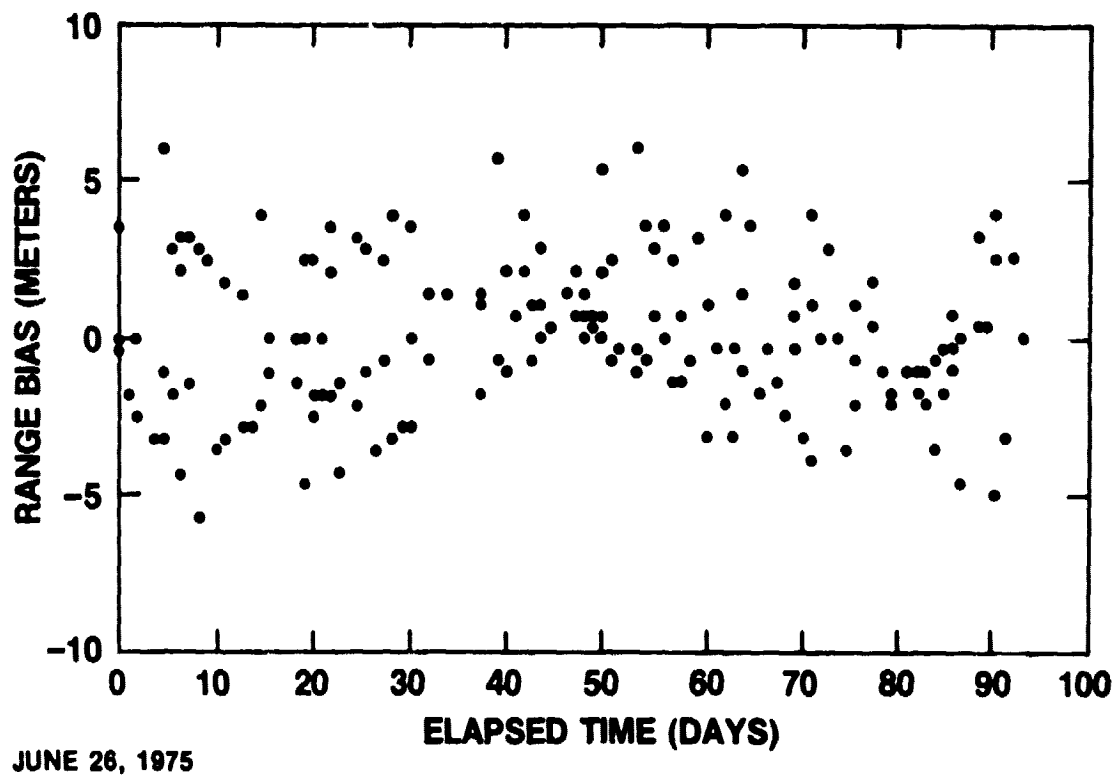


Figure 7. Starlette Ninety Day Orbit Range Biases at the Arequipa, Peru Laser Station

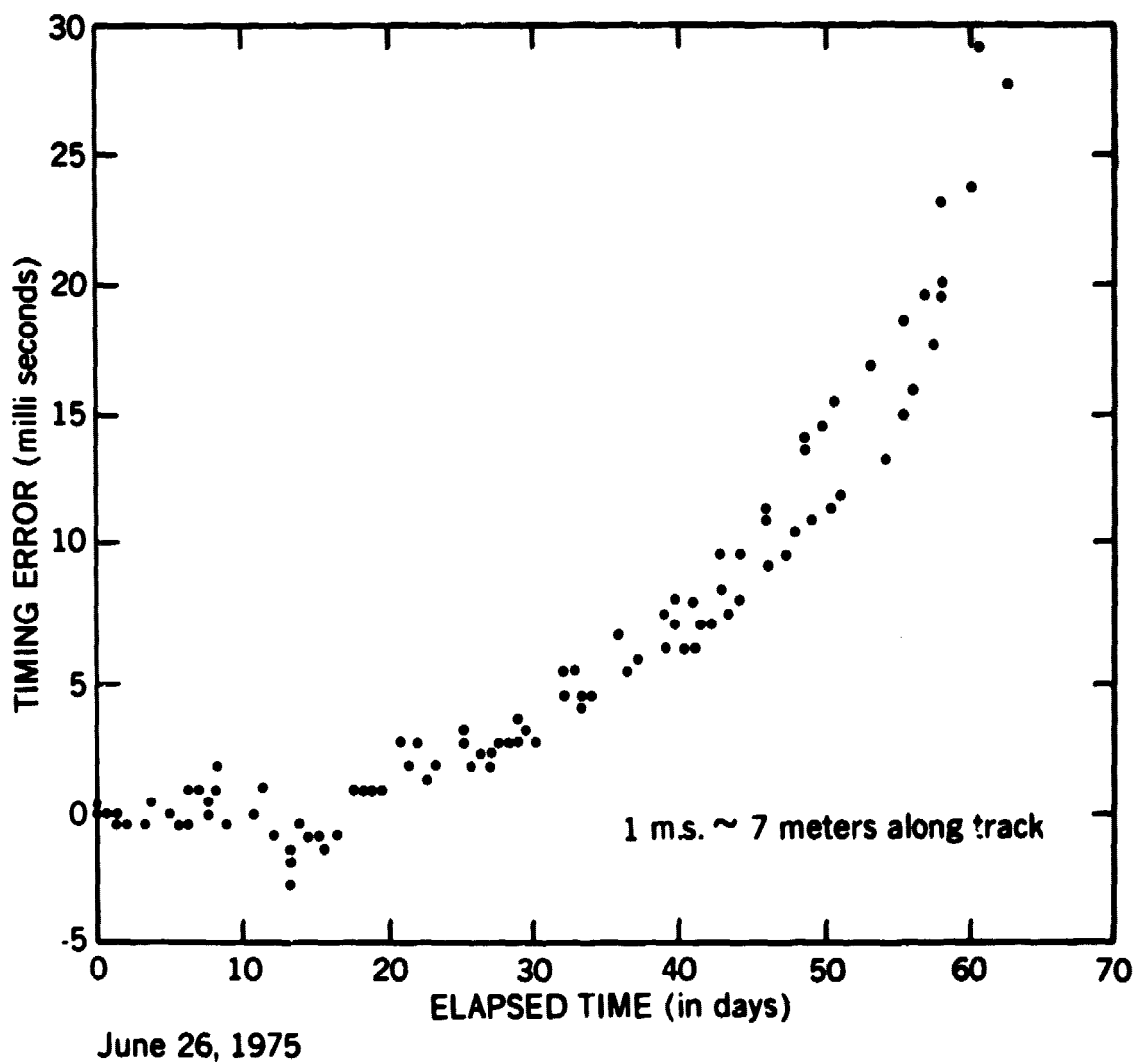
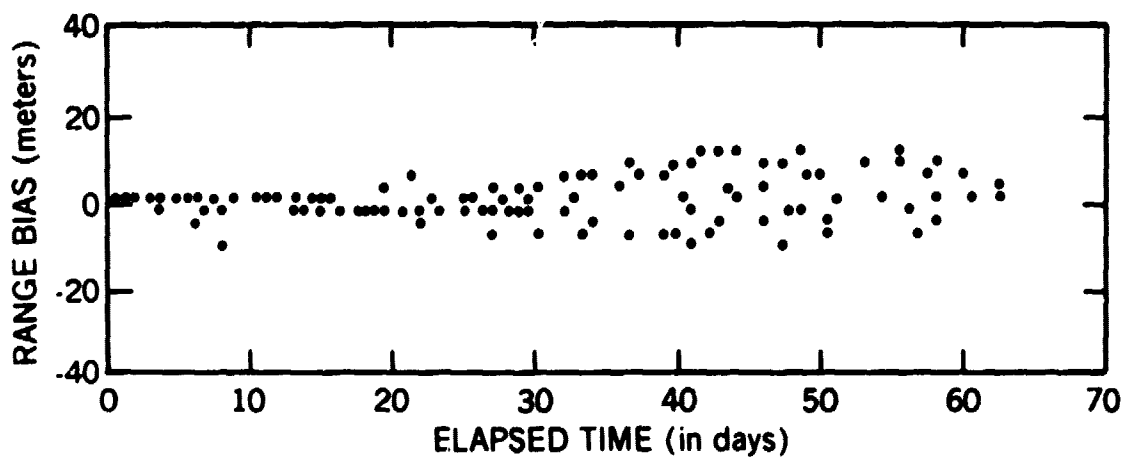


Figure 8. Starlette Orbit Prediction Based Upon A Five Day Arc Timing Errors At The Arequipa, Peru Laser Station



June 26, 1975

Figure 9. Starlette Orbit Prediction Based Upon a Five Day Arc  
Range Biases At The Arequipa, Peru Laser Station

**Table 1****Starlette Gravity Model Comparison RMS Fits for 5-Day Orbits**

<b>Epoch (1975)</b>	<b>No. of Observations *</b>	<b>RMS Fit (Meters)</b>	
		<b>GEM-7</b>	<b>PGS-ST4</b>
<b>June 11</b>	<b>1500</b>	<b>9.5</b>	<b>1.1</b>
<b>June 16</b>	<b>2300</b>	<b>7.6</b>	<b>1.1</b>
<b>June 21</b>	<b>2000</b>	<b>10.5</b>	<b>1.7</b>
<b>June 26</b>	<b>1200</b>	<b>10.5</b>	<b>2.1</b>

\*Approximate.

**Table 2****Gravity Model Effects on Orbit Overlap RMS Differences (Meters)  
(5-Day Orbits With a 2.5 Day Overlap)**

<b>Epoch (1975)</b>	<b>Radial</b>		<b>Cross Track</b>		<b>Along Track</b>	
	<b>GEM-7</b>	<b>PGS-ST4</b>	<b>GEM-7</b>	<b>PGS-ST4</b>	<b>GEM-7</b>	<b>PGS-ST4</b>
<b>June 11</b>	<b>1.4</b>	<b>0.4</b>	<b>1.6</b>	<b>1.5</b>	<b>9.6</b>	<b>1.8</b>
<b>June 16</b>	<b>1.1</b>	<b>0.2</b>	<b>2.5</b>	<b>0.2</b>	<b>4.8</b>	<b>0.9</b>
<b>June 21</b>	<b>0.8</b>	<b>0.2</b>	<b>1.6</b>	<b>0.9</b>	<b>4.1</b>	<b>1.4</b>
<b>June 26</b>	<b>3.0</b>	<b>0.2</b>	<b>1.2</b>	<b>0.5</b>	<b>18.4</b>	<b>2.0</b>

Table 3

Statistics by Station for Starlette 90 Day Arc  
May 1 to August 1, 1975

Station	No. of Obs.	No. of Passes	Mean (Meters)	RMS (Meters)
Goddard (7063)	3,490	42	-0.07	3.2
Grand Turk (7068)	1,142	26	0.00	2.6
Bermuda (7067)	353	8	0.46	2.2
Arequipa (9907)	8,080	172	-0.40	4.8
Olifantsfontein (9902)	6,732	162	-0.47	4.3
Natal (9929)	1,049	43	-0.40	4.3
Mt. Hopkins (9921)	953	31	0.33	4.2
Dionysos (9940)	138	35	0.35	5.1
Canary Isl. (7819)	621	23	-0.99	4.8
Overall	22,308	542	—	4.3